Advances in Aircraft and Spacecraft Science, *Vol. 4, No. 1 (2017) 81-91*
DOI: http://dx.doi.org/10.12989/aas.2017.4.1.081

Design of a morphing flap in a two component airfoil with a droop nose

Antonio Carozza*

Dipartimento di Meccanica dei Fluidi, Centro Italiano Ricerche Aerospaziali, CIRA, Capua, via Maiorise, 81043, Italy

(Received January 6, 2016, Revised May 26, 2016, Accepted May 27, 2016)

Abstract. The performances of lifting surfaces are particularly critical in specific flight conditions like takeoff and landing. Different systems can be used to increase the lift and drag coefficients in such conditions like slat, flap or ailerons. Nevertheless they increase the losses and make difficult the mechanical design of wing structures. Morphing surfaces are a compromise between a right increase in lift and a reduction of parts movements involved in the actuation. Furthermore these systems are suitable for more than one flight condition with low inertia problems. So, flap and slats can be easily substituted by the corresponding morphing shapes. This paper deals with a genetic optimization of an airfoil with morphing flap with an already optimized nose. Indeed, two different codes are used to solve the equations, a finite volume code suitable for structured grids named ZEN and the EulerBoundary Layer Drela's code MSES. First a number of different preliminary design tests were done considering a specific set of design variables in order to restrict the design region. Then a RANS optimization with a single design point related to the take-off flight condition has been carried out in order to refine the previous design. Results are shown using the characteristic curves of the best and of the baseline reported to outline the computed performances enhancements. They reveal how the contemporary use of a morphing acting on the nose of the main component and the trailing edge of the flap drive towards a total not negligible increment in lift.

Keywords: deflection; genetic algorithm; gap; Euler; morphing; overlap; RANS

1. Introduction

The idea of acting geometry variations to meet the best requirements at several flight regimes, has been pursued since the beginning of flight history, movable parts like ailerons, flaps, equilibrators represent just some of the most common solutions aimed at extending aircraft flight envelope, Anderson (2011). Anyway, despite of related advantages, both weight increase caused by actuators, and discontinuities induced onto aerodynamic surfaces, penalize these solutions. Thus, several alternative design approaches have being taken into account; among the others, one recalls the morphing oriented design, that envisages actuation strategies able to produce smooth and, at the same time, significant geometry variations. The morphing mechanism is useful to realize strong variations of curvature without to adopt slat and flaps with their related variations of gap overlap and deflections. Morphing aircraft structures can in this manner significantly enhance aircraft

∗Corresponding author, Ph.D., E-mail: a.carozza@cira.it

http://www.techno-press.org/?journal=aas&subpage=7 ISSN: 2287-528X (Print), 2287-5271 (Online)

performances. Several studies are carried out in the past years on the morphing in order to find the best solution for this kind of technologies in terms of shape and actuating strategies. A good summary of such studies are reported in Barbarino, Bilgen *et al.* (2011). Furtherly a number of algorithms are used in the past years to perform a design of morphing flaps, from the conjugate gradient methods to the evolution methods, genetic or other. In aerospace engineering, different methods were applied to the design of a morphing flap as illustrated by Quagliarella (2003). It is also to be considered also that most of the morphing technologies or concepts assume the existence of an appropriate flexible skin. Thill, Etches *et al.* (2008) performed a comprehensive review of flexible skins and considered various novel material systems concepts and technologies. The design of flexible skins is challenging and has many conflicting requirements. The skin must be soft enough to allow shape changes but at the same time it must be stiff enough to withstand the aerodynamic loads and maintain the required shape/profile. This requires thorough trade-off design studies between the requirements. Furthermore, the use of morphing core sandwich structures covered by compliant face sheet has been investigated by (Olympio and Gandhi 2010a, b).

The design of the morphing surfaces has been until now conducted considering just a single specific part of the lifting surfaces. Furthermore, the various typologies of design adopted in the past wing optimizations involving morphing mechanisms did not consider the difficulties the RANS codes can meet when the flow field around a dropped nose two component airfoil is investigated at an high angle of attack, almost near the stall. Taking into account these difficulties, the authors believe that a double optimization regarding both the leading edge and the trailing edge can be useful to understand how much the high lift capabilities of a modern wing can be increased with morphing surfaces and limiting computational costs and times. At this aim, a RANS genetic optimization has been performed on the flap considering a single design point corresponding to a critical flight condition such as the take-off phase of the flight envelope. The solver authors used was a finite volume code with different available turbulence models capable to solve Reynolds averaged Navier Stokes equations on structured multi block grids and using multi grid and multi level techniques. In particular three different levels of grid refinement have been considered during each individual fitness evaluation. Typical values of mutation rate and crossover rate have been used. At the end, angle of attack and lift coefficient changed showing a particularly interesting stability increase and a not too bad increase in drag. So, it has been possible to increase the lift coefficient avoiding the use of more separated wetted surfaces both on the aft part and on the rear part of the wing.

2. Theory and numerical approach

In order to investigate any possible shape and settings variations to apply on the baseline geometry an inhouse geometry handler named *WG2AER* was used. This code is able to move any component of the airfoil applying to it both shape and setting modes by means of two files of input. One contains the shape and setting functions to be applied to a component and the other instead contains the weights by which the optimizer can decide in which directions increase or decrease the aforementioned modes. A multi-component airfoil design procedure, based on the CIRA in-house developed *GA-ME* (Multi-Objective Genetic Algorithm for Multi Element Airfoils) optimizer is used to carry out the design work. The *GA-ME* optimization code is interfaced with solvers of different nature for objective function evaluation. This code has been widely validated as reported in many publications like in Vicini and Quagliarella (1997). Depending on problem difficulty and on

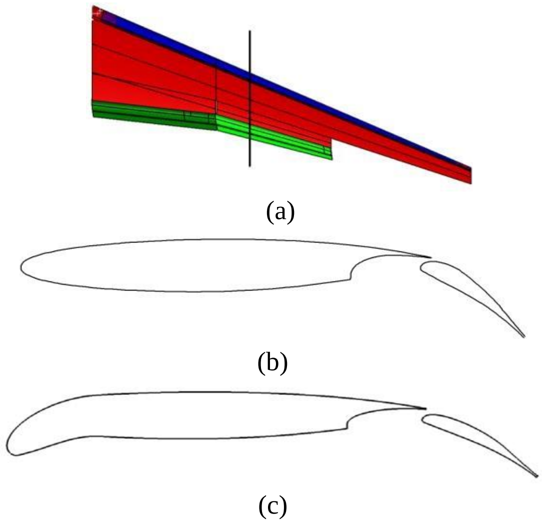

Fig. 1 HARLS Wing (a), section with and without droop nose (b)-(c)

the design target, the optimization procedure can use either an Euler-Boundary layer Prof. Drela's MSES code (Drela 2007) or the in-house developed RANS ZEN code by Amato, Paparone *et al.* (1999), capable of solving Euler and Navier- Stokes equations around very complex, threedimensional configurations.

3. Problem definition

In this article a genetic optimization has been done on a two component airfoil capable of morphing. The geometry under investigation is shown in Fig. 1. The initial shape is derived from the HARLS 3D model as depicted in Fig. 1. A stream wise section was extracted from that wing and used as the clean input geometry for the optimization of droop nose. The final optimized shape provided by DLR is the baseline shape considered in this work.

The baseline configuration chosen to carry out the 2D design activities is derived from the high lift HARLS wing provided by AIRBUS, as modified by Kühn (2010), as shown in Fig. 1. As the reader can see, the geometry has a starting, already optmized, morphed droop nose, while the flap is a classic flap and is the target of the present morphing genetic optimization. The aim of the full optimization work was to increase the lift of the baseline geometry at the stall and if possible increase also the stall angle of attack. So it was decided to consider just one design point as follows:

1. Mach M = 0.15
2. Reynolds number Re = 7.0E+06
3. AoA = 8°

4. Flow solvers

The RANS, Reynolds Averaged Navier Stokes, equations are adopted as the flow field governing equations and have essential role in determination of the objective function.

The following momentum conservation was used along with the continuity equation

$$\rho\left(\frac{\partial v}{\partial t} + v \cdot \nabla v \right) = -\nabla p + \nabla \cdot T + f + \rho g \tag{1}$$

To modeling heat transfer, the energy equation is solved in the form shown below

$$\frac{\partial(\rho E)}{\partial t} + \nabla \cdot (v(\rho E + p)) = \nabla \cdot (k_{eff} \nabla T - \sum_j h_j J_j + (\tau \cdot v)) + S_h \tag{2}$$

The solver used for the calculations is ZEN, see the articles by Catalano and Amato (2001), Amato and Catalano (2000), Marongiu, Catalano *et al*. (2004). ZEN is a multi-block RANS software that solves RANS equations using a modified explicit multistage Runge-Kutta time-stepping scheme, see also Ferziger and Peric (1996).

A finite volume technique and second order central differencing in space are applied to the integral form of the Navier- Stokes equations. The Jameson-Schmidt-Turkel scheme, see the article by Jameson (1991), with adaptive coefficients for artificial dissipation is used to prevent odd-even oscillations and to allow for the clean capture of shock waves and contact discontinuities.

In addition, local time stepping, implicit residual smoothing, and the multi-grid method can be applied to accelerate convergence to steady-state solutions. The k-ω TNT two equations model by Kok (2000) was used to model the Reynolds stresses, see also Wilcox (1994). The system allows to perform all the steps required to get an aerodynamic solution around complex geometry defined as a CAD model:

- generation of a multi-block structured grid;
- specification of the flow model and the boundary conditions;
- computation of the flow solution;
- selection of the visualization data and domain
- analysis of the flow solution

The system comprises a specific domain modeler and grid generator (ENDOMO and ENGRID), a steady/unsteady flow solver (ZEN/UZEN) and a set of utilities for files manipulation and convergence plotting.

The function to minimize has been defined as follows for the only design point taken into account

$$F(\underline{x}) = -C_l + W \times P^2 (C_d - C_{d,baseline}) \tag{3}$$

Where $\underline{x}=[\Delta_{gap} \quad \delta\theta_{FLAP} \quad \Delta x_{FO} \quad \alpha_{FLAP}]$ is the vector of the design variables shown in Fig. 3 while C_l, C_d and $C_{d,baseline}$ are the lift and drag coefficients while W is the weight factor associated to the

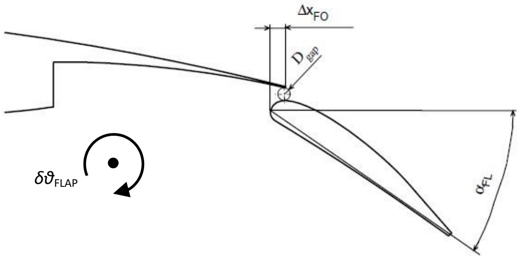

Fig. 2 Degrees of freedom for flap

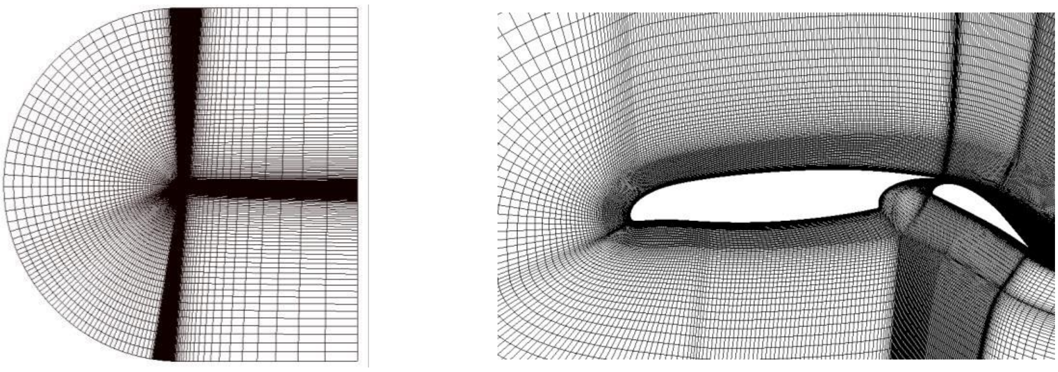

(a) (b)

Fig. 3 Mesh grid overview and detail on the body

square penalty involving the drag, chosen equal to 10^3 based on the first phase done with the Euler optimization.

5. Results and discussion

Before the optimization of the morphing airfoil was performed, the non-morphing case was computed. A Navier-Stokes tuning has been considered preliminarily on a structured grid with three levels of refinement, for about 118496 cells on the finer level and 62 blocks and assuring a right refinement overall in the proximity of the body and a Far field distance of 30 chord size, as you can see in Figs. 3(a)-(b).

In Fig. 4 a sample of the convergence values of reference is shown to guarantee the RANS solution rate. The geometry is next passed to the CFD toolbox which generates the computational grid generation, executes the CFD computation, extracts the relevant data from the CFD solution and sends the relevant information to the optimizer which builds up the objective function value for such an individual. The objective function has been formulated considering both a contribution of lift coefficient and a penalty function applied to the drag coefficient. The center of rotation for the morphing has been moved in a range of 40-60 % of the chord size, while the allowed deflection of the flap rear part was around 10 degrees. The fitness function variation has been of about 0.15 with 160 generations. A smoothing post-process of the RANS optimum has been done in order to avoid jumps in the pressure distribution on the flap that could generate problems from a structural point of view. Finally, the polar curves of the baseline and the best are reported and the related table of values in Figs. 7-9 and Table 1. The optimization process has been carried out considering a first phase in which a tuning of genetic algorithm has been performed considering several fitness function mathematical expressions and different ranges for the design variables. A second phase of design is then performed in order to refine more deeply the lift enhancement for the two component airfoil with morphing flap.

In Fig. 4 a sample of the convergence values of reference is shown to guarantee the RANS solution rate. The geometry is next passed to the CFD toolbox which generates the computational grid generation, executes the CFD computation, extracts the relevant data from the CFD solution and sends the relevant information to the optimizer which builds up the objective function value for

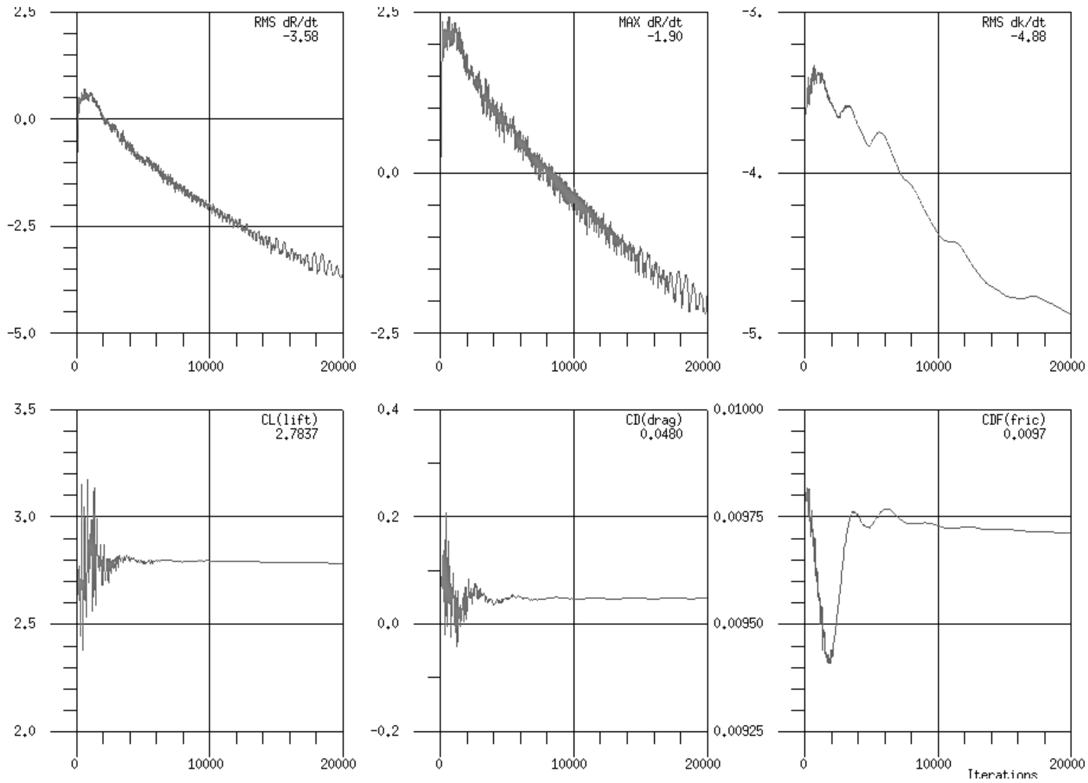

Fig. 4 Residuals convergence for grid topology validation

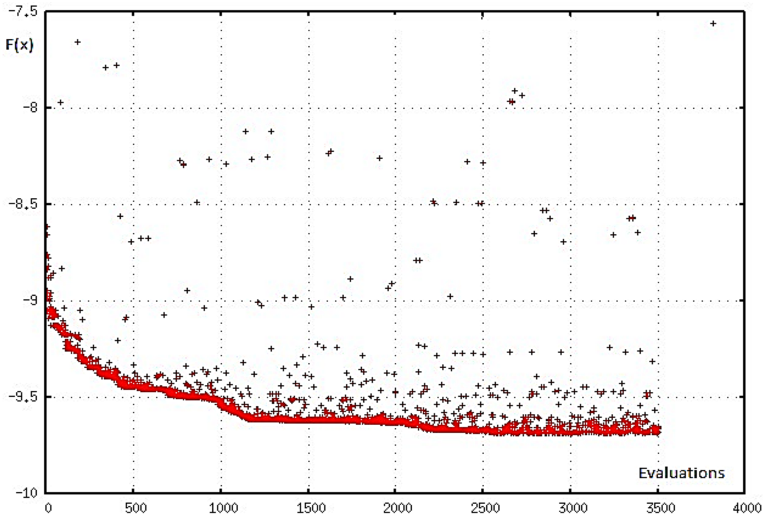

Fig. 5 Tuning optimization Eulerian run results with 3 design points, 250 generations

such an individual. The objective function has been formulated considering both a contribution of lift coefficient and a penalty function applied to the drag coefficient. The center of rotation for the morphing has been moved in a range of 40-60 % of the chord size, while the allowed deflection of

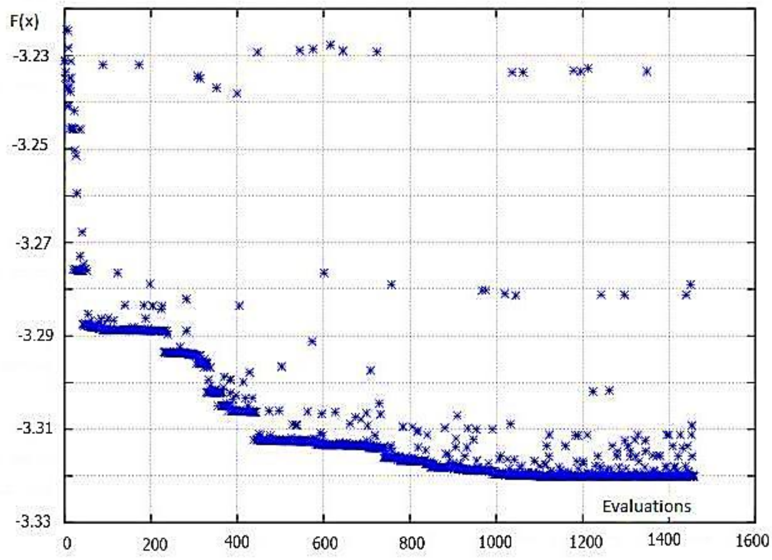

Fig. 6 RANS optimization history

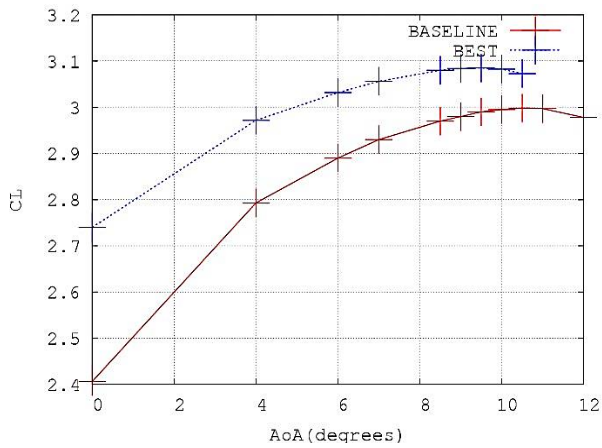

Fig. 7 C_l-α curves for baseline and best geometries

the flap rear part was around 10 degrees. The fitness function variation has been of about 0.15 with 160 generations. A smoothing post-process of the RANS optimum has been done in order to avoid jumps in the pressure distribution on the flap that could generate problems from a structural point of view. Finally, the polar curves of the baseline and the best are reported and the related table of values in Figs. 7-9 and Table 1.

The optimization process has been carried out considering a first phase in which a tuning of genetic algorithm has been performed considering several fitness function mathematical expressions and different ranges for the design variables. A second phase of design is then performed in order to refine more deeply the lift enhancement for the two component airfoil with morphing flap.

Different preliminary multipoint optimization runs were performed with different objective functions in order to restrict the design region of research. P^2, see Eq. (1), indicates a square penalty set on a triplet of drag coefficients. Geometrical constraints on gap and overlap ranges are considered and flap trailing edge deformation up to 12.5% of clean wing chord size is allowed.

The design variables are flap deformation, flap *x* and *y* position and rotation, angle of attack. With this Euler-Boundary Layer design process, the following shift in the angles of attack and lift increase are achieved:

√ $\Delta\alpha$ = -2.5°
√ ΔC_l = +0.0289C_l = +0.1

A sample of convergence history for the aforementioned optimization runs is reported in Fig. 5.

This first phase has allowed to investigate the solutions region and detect a subzone particularly interesting for our scopes. Euler Boundary Layer Drela's MSES v2.9 code has been preliminary used to perform a gross design in order to restrict the design region. Eight optimization runs have been done and were necessary to really restrict the optimum investigation region. Then a single point RANS genetic optimization has been carried out in order to detect the optimum configuration for the morphing flap, see a sample of convergence in Fig. 6. The flight condition at which the optimization process has been carried out has been chosen in order to increase the polar curves. It considers an angle of attack of 8° and Mach and Reynolds numbers equal to 0.17 and 7 Millions, respectively. It should guarantee a greater lift than the baseline when the aircraft approaches the landing or starts the take-off flight phase. A population of 16 elements has been considered for each

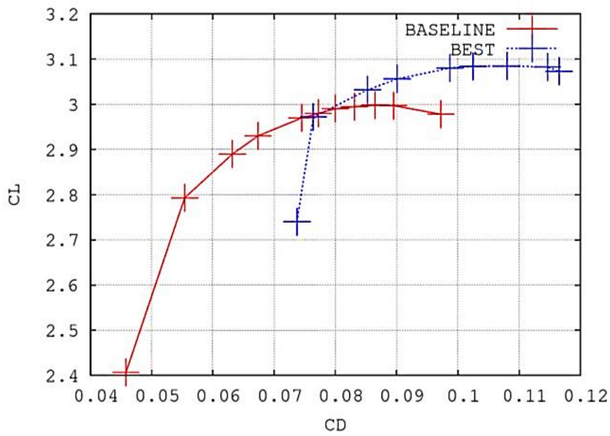

Fig. 8 C_l-C_d curves for baseline and best geometries

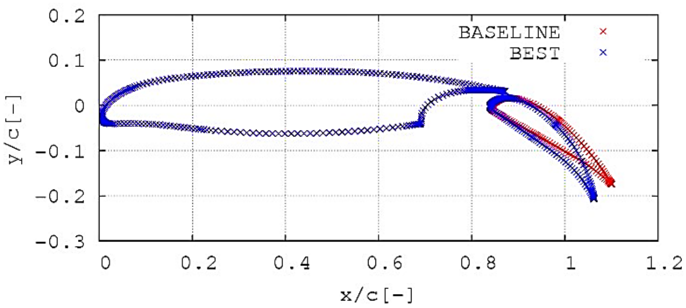

Fig. 9 Baseline and best geometries points

Table 1 Design variables initial and optimized values

Flap morphing centre position (*x/c*)	Δgap	$\delta\theta_{\text{Flap}}$	Δx_{FO}	αFLAP
0.60	0.0235	10.23	0.113	2.5
0.60	0.0325	11.52	0.135	5.3

generation. This choice for parameters of the genetic algorithm has been done considering the CPU consumption that such a run can involve and also because of the licences of the grid generator available during the computations. So, after a number of preliminary tests the definitive optimization run has been launched on a 64 core machine provided with a Red Hot UNIX system.

It is to be said that with a single design point applying a mechanism of morphing on the flap allows to increase the lifting performances for all the range of angles of attack. This can be achieved with an important increment of drag that, as you can see in Fig. 8, is around the 85% of the start value. The stability of the best configuration is over the initial value. This is likely due to an increase of total curvature without a significant variation of the gap and overlap.

In Table 1, the Euler and RANS design variable variations are reported to confirm what has been stated before. Indeed, gap and overlap variations are under 0.1 while α_{Flap} and $\delta\theta_{Flap}$ change themselves relevantly. This can be explained considering the drag increase that in the zone of separation between the two components is important. In other words the airfoil behaves as a one component airfoil with a greater curvature and this is intuitive. It also is interesting to notice how the center of rotation for morphing part of the flap is positioned towards the trailing edge. This is because the edge of separation on the wake must be reduced as much as possible to increase effectively the aerodynamic performances of the whole system. Other researchers in recent years have focused their attention on the design of compliant morphing mechanisms. Shili, Wenjie *et al*. (2008), Secanel, Suleman *et al*. (2006), introduced a systematic approach to design compliant structures to perform required shape changes under distributed pressure loads. The distributed compliant mechanism was optimized using a GA. A direct search method was used to locally optimize the dimension and input displacement after the GA optimization. The resultant structure achieved a 9.3° angle change, which was also validated using a prototype.

6. Conclusions

In this study, a two-component airfoil optimization has been performed by using a genetic algorithm with hybrid capabilities. Two morphing mechanisms have been considered, one for the nose and one other for the flap trailing edge. Starting from an already optimized airfoil on the nose, in this article only the flap morphing has been investigated aerodynamically. The design process has been performed as follows:

- an Euler simplified optimization has been carried out to restrict the optimum region of search
- a RANS genetic design has been accomplished to refine the previous gross design process.

It has to be said that a single design point revealed sufficient to increase the lift coefficient changing both the shape and the position of the flap.

It has to be said that the achieved optimal shape:

- needs to be compared with the one that effectively can be obtained with the proper kinematics

• it represents a relevant improvement with respect to the baseline
• should be validated by means of tests in a proper wind tunnel.

References

Amato, M. and Catalano, P. (2000), “Non Linear *κ-ε* turbulence modeling for industrial applications”, *ICAS 2000 Congress*, Harrogate, UK.

Amato, M., Paparone, L., Catalano, P. and Puoti, V. (1999), “Zen flow solver, Zonal Euler Navier- stokes flow solver user guide”, Technical Report, CIRA, Centro Italiano Ricerche Aerospaziali.

Anderson, J.D. Jr (2011), *Fundamentals of aerodynamics. McGraw-Hill Higher Education*, 3rd edition.

Barbarino, S., Bilgen, O., Ajaj, R.M., Friswell, M.I. and Inman, D.J. (2011), “A review of morphing aircraft”, *J. Intell. Mater. Syst. Struct*., **22**, 823-877.

Catalano, P. and Amato, M. (2001), “Assessment of κ-ω turbulence modeling in the CIRA flow solver ZEN”, *ECCOMAS 2001 Conference*, Swansea, Wales.

Ferziger, J. H. and Peric, M. (1996), *Computational Methods for Fluid Dynamics*, Springer-Verlag, Berlin & Heidelberg.

Jameson, A. (1991), “Time dependent calculations using multigrid, with applications to unsteady flows past airfoils and wings”, *AIAA Paper*, AIAA 10th Computational Fluid Dynamics Conference, Honolulu, HI, June.

Kok, J. (2000), “Resolving the dependence on free-stream values for the *κ-ω* turbulence model”, *AIAA J.*, **38**(7), 1292-1295.

Kühn, T. (2010), “Aerodynamic optimization of a two-dimensional two-element high lift airfoil with a smart droop nose device”, *1st EASN Association Workshop on Aerostructures*, Paris, France

Mark, D. (2007), *A User’s Guide to MSES 3.05*, MIT Department of Aeronautics and Astronautics, July.

Marongiu, C., Catalano, P., Amato, M. and Iaccarino, G. (2004), “U-ZEN: a computational tool solving U-RANS equations for industrial unsteady applications”, *34th AIAA Fluid Dynamics Conference*, Portland (Or), AIAA Paper 2004-2345.

Olympio, K.R. and Gandhi, F. (2010a), “Flexible skins for morphing aircraft using cellular honeycomb cores”, *J. Intel. Mater. Syst. Struct.*, **21**, 1719-1735.

Olympio, K.R. and Gandhi, F. (2010b), “Zero poisson’s ratio cellular honeycombs for flex skins undergoing one-dimensional morphing”, *J. Intel. Mater. Syst. Struct.*, **21**, 1737-1753.

Quagliarella, D. (2003), “Airfoil design using Navier-Stokes equations and an asymmetric multi-objective genetic algorithm”, *Evolutionary Methods for Design, Optimization and Control Applications to Industrial and Societal Problems*, International Center for Numerical Methods in Engineering (CIMNE), Barcelona, Spain.

Secanell, M., Suleman, A. and Gamboa, P. (2006), “Design of a morphing airfoil using aerodynamic shape optimization”, *AIAA J.*, **44**(7), 1550-1562.

Shili, L., Wenjie, G. and Shujun, L. (2008), “Optimal design of compliant trailing edge for shape changing”, *Chin. J. Aeronaut.*, **21**, 187-192.

Thill, C., Etches, J., Bond, I., Potter, K. and Weaver, P. (2008), “Morphing skins”, *Aeronaut. J.*, **112**, 117-139.

Vicini, A. and Quagliarella, D. (1997), “Inverse and direct airfoil design using a multi-objective genetic algorithm”, *AIAA J.*, **35**(**9**), 1499-1505.

Wilcox, D.C. (1994), *Turbulence Modeling for CFD*, DCW Industries Inc., La Canada, Los Angeles, California.

EC

Nomenclature

D_{gap}	Gap distance
$\delta\theta_{\mathrm{FLAP}}$	Flap TE deflection
Δx_{FO}	Overlap distance
α_{FLAP}	Flap rotation
DP	Design Point
W	weight factor
P^2	square penalty
TE	trailing edge
AoA	angle of attack [°]
GA-ME	CIRA genetic algorithm for multi-element airfoil optimization
WG2AER	CIRA geometry handler
C_l	lift coefficient
C_d	drag coefficient
C_m	pitch moment coefficient
HARLS	High Aspect Ratio Low Sweep